



저작자표시-동일조건변경허락 2.0 대한민국

이용자는 아래의 조건을 따르는 경우에 한하여 자유롭게

- 이 저작물을 복제, 배포, 전송, 전시, 공연 및 방송할 수 있습니다.
- 이차적 저작물을 작성할 수 있습니다.
- 이 저작물을 영리 목적으로 이용할 수 있습니다.

다음과 같은 조건을 따라야 합니다:



저작자표시. 귀하는 원저작자를 표시하여야 합니다.



동일조건변경허락. 귀하가 이 저작물을 개작, 변형 또는 가공했을 경우에는, 이 저작물과 동일한 이용허락조건하에서만 배포할 수 있습니다.

- 귀하는, 이 저작물의 재이용이나 배포의 경우, 이 저작물에 적용된 이용허락조건을 명확하게 나타내어야 합니다.
- 저작권자로부터 별도의 허가를 받으면 이러한 조건들은 적용되지 않습니다.

저작권법에 따른 이용자의 권리는 위의 내용에 의하여 영향을 받지 않습니다.

이것은 [이용허락규약\(Legal Code\)](#)을 이해하기 쉽게 요약한 것입니다.

[Disclaimer](#)

February 2013

Master's Thesis

A Study on the Mechanical Characteristics of Friction Stir Welded Joint for Thin Ferritic Stainless Steel

Graduate School of Chosun University

Department of Naval Architecture and
Ocean Engineering

Kyoung-Hak Kim

A Study on the Mechanical Characteristics of Friction Stir Welded Joints for Thin Ferritic Stainless Steel

마찰교반접합기술을 이용한 박판 페라이트계 스테인리스강
접합부의 기계적 특성에 관한 연구

February 25, 2013

Graduate School of Chosun University

Department of Naval Architecture and
Ocean Engineering

Kyoung-Hak Kim

A Study on the Mechanical Characteristics of Friction Stir Welded Joints for Thin Ferritic Stainless Steel

Advisor : Professor Han-Sur Bang

A Thesis submitted for the degree of
Master of Engineering

October 2012

Graduate School of Chosun University

Department of Naval Architecture and
Ocean Engineering

Kyoung-Hak Kim

Kyoung-Hak Kim's master thesis certified.

Committee Chair Chosun Univ. Prof. Hee-Seon Bang

Member Chosun Univ. Prof. Han-Sur Bang

Member Chosun Univ. Prof. Je-Woong Park

November 2012

Graduate School of Chosun University

CONTENTS

List of Tables	III
List of Figures	IV
Abstract	VI

Chapter 1. Introduction

1. 1 Research Background and Purpose	1
1.1.1 Application of FSW	4
1.1.2 Application of stainless steel in industries	6
1. 2 Research Methodology	7

Chapter 2. Theoretical Background

2. 1 Principle and Characteristics of FSW	8
2.1.1 Principle of FSW	8
2.1.2 Characteristic microstructure of FSW	10
2.1.3 Generation and flow of heat	12
2.1.4 Advantages and limitations of FSW	13
2. 2 Classification of Stainless Steel	15

Chapter 3. Experimental Method of Friction Stir Welding Process

3. 1 Experimental Details	18
3.1.1 Experimental equipment	18

3.1.2 Objective material	20
3.1.3 Description of tool material and shape	22
3. 2 Experimental Procedure	23
3. 3 Mechanical Evaluation	25
3.3.1. Tensile test	25
3.3.2. Hardness test	27
3. 4 Metallurgical Evaluation	29
3. 5 Temperature Measurement	31
Chapter 4. Results and Discussions	
4. 1 Bead Profiles	33
4. 2 Mechanical Characteristics	34
4.2.1. Tensile strength	35
4.2.2. Hardness	38
4. 3 Metallurgical Characteristics	39
4. 4 Measured Temperature History	45
Chapter 5. Conclusion	39
Reference	47

List of Tables

Table 3.1	Chemical compositions and mechanical properties	21
Table 3.2	Configuration of welded specimen	21
Table 3.3	Chemical compositions and mechanical properties of tool	22
Table 3.4	Welding parameters of FSW	24
Table 3.5	Geometry of tensile test specimen	26
Table 3.6	Hardness testing condition	28
Table 4.1	Bead profiles of welds for various travel speed in different rotation speed	33
Table 4.2	Tensile strength and fractured specimen after tensile test for various travel speed in different rotation speed	36

List of Figures

Fig. 1.1	Application of FSW to stainless steel	3
Fig. 1.2	Application of FSW in industries	5
Fig. 1.3	Application of stainless steel in industries	6
Fig. 2.1	Schematic diagram of FSW	8
Fig. 2.2	Microstructural regions in FSW welds	10
Fig. 2.3	Classification of ferritic stainless steels	15
Fig. 2.4	Classification of austenitic stainless steels	16
Fig. 2.5	Classification of martensitic stainless steels	17
Fig. 3.1	Specifications of FSW system	19
Fig. 3.2	Experimental set-up for FSW	19
Fig. 3.3	Dimensions and shape of tool	22
Fig. 3.4	Tensile test machine	26
Fig. 3.5	Vickers hardness test scheme and machine	28
Fig. 3.6	Optical microscope	29
Fig. 3.7	Common thermocouple temperature ranges	31
Fig. 3.8	Set-up for temperature measurement	32
Fig. 3.9	Thermocouple positions on workpiece	32
Fig. 4.1	Tensile test specimens	35
Fig. 4.2	Comparison of tensile strength of FSW welds with travel speed	35
Fig. 4.3	Comparison of stress-strain curve of FSW welds with travel speed	36
Fig. 4.4	Stress-strain curve for end part of FSW welded specimen	37
Fig. 4.5	Hardness distributions of FSW welds	38
Fig. 4.6	Optical microstructure of FSW welds	40

Fig. 4.7	SEM image of FSW welds	42
Fig. 4.8	SEM observation of fracture surface after tensile test with travel speed	43
Fig. 4.9	SEM observation of fracture surface after tensile test for end part of welded specimen	44
Fig. 4.10	Temperature history of FSW welds	45
Fig. 4.11	Comparison of temperature history of FSW welds and GTAW welds	46

ABSTRACT

마찰교반접합기술을 이용한 박판 페라이트계 스테인리스강 접합부의 기계적 특성에 관한 연구

Kim Kyoung Hak

Advisor : Prof. Bang Han-sur, Ph.D.

Department of Naval Architecture and
Ocean Engineering,

Graduate School of Chosun University

세계적으로 대기오염 및 지구온난화 그리고 자원고갈로 인하여 21세기를 맞이한 현대사회의 각종 산업분야에서 최대의 핵심 과제는 “친환경적 녹색성장”일 것이다. 이에 따라 각종 산업분야에서는 환경보호 및 에너지 절감에 대한 요구를 만족하기 위하여 경량부재의 적용 및 부재재질의 두께 감소 등 녹색 기술에 집중하고 있다. 또한 세계적인 경제 발달과 더불어 삶의 질의 향상 및 편의를 위해 많은 종류의 가전제품이 개발 및 출시되고 있으며 3대 그린가전 중의 하나인 세탁기의 경우 그 기술 개발속도가 빠르게 이루어지고 있으며, 세계적인 수요 또한 꾸준히 증가하고 있는 추세이다.

스테인리스강의 경우 표면이 미려하고 부식에 대한 저항성이 우수한 특수강으로 내식성, 내구성, 내화성 등 제품의 고급화를 요구하는 자동차, 가전제품의 수요산업에서 사용이 크게 증가하고 있다. STS430J1L의 경우 기존 STS430에 Cu, Nb를 첨가하여 내식성, 성형성, 용접성 및 고온특성이 우수하기 때문에 자동차, 가전제품, 철강, 플랜트 등의 합금강 산업 분야 전반에 걸쳐 사용되고 있으며 그 활용도가 더욱 증가하고 있다.

그러나 기존 스테인리스강 용접의 경우 일반적으로 MIG 및 TIG와 같은 불활성 가스를 이용한 용융용접법을 적용하고 있으며, 이러한 경우 고온용융에 따른 용접부의 균열 및 변형, 잔류응력, 기공, 산화 등 용접결함 뿐만 아니라 접합부에 의한 탄화크롬 석출이 발생하여 내부식성이 저하되어 접합부의 부식으로 고품질의 접합부를 얻을 수 없게 되며 실온에서 연성과 인성이

감소하는 단점이 있어 스테인리스강 접합에 새로운 다른 열원의 필요성이 요구되고 있다.

이러한 문제점 등을 개선한 접합방법으로 1981년 영국의 용접연구소(The Welding Institute of the United Kingdom, 이하 TWI)에서 개발한 마찰교반 접합(Friction Stir Welding, 이하 FSW)은 용접이하에서 고상 상태의 접합공정으로 회전하는 Tool을 피접합체에 삽입하여 접합부에 충분한 마찰열과 강한 소성변형이 발생하여 매우 미세한 재결정 조직 및 우수한 기계적 특성을 얻을 수 있다고 알려져 있다. 이러한 공정은 기존 용융용접공정과 비교하여 용접에 의한 변형이 적고 비소모성 접합방법일 뿐만 아니라 용접결함, 흠, 유해광선의 발생이 없어 환경친화형 접합방법으로 각광을 받고 있다.

하지만, 이러한 장점에도 불구하고 박판재 접합에 있어서 국내·외 산업 및 응용분야에서는 대부분 용융용접법(TIG 및 MIG)을 이용하여 구현되고 있으며, 마찰교반접합을 이용한 박판재 접합에 관한 연구 및 적용은 거의 전무한 실정이다.

따라서 본 연구에서는 내식성, 성형성, 용접성 및 고온특성이 우수하여 공업용으로 사용되고 있는 STS430J1L을 새로운 열원으로 마찰교반접합기술을 이용하여 접합기구상의 특성상 박판접합에 있어서 프로브(Probe)가 없는 타입의 단순한 환봉형태의 공구(Tool)를 사용하였고, 접합부의 미세조직 관찰(OM 및 SEM) 및 인장, 경도시험을 통하여 기계적 특성을 평가하였다. 또한 접합성을 평가하여 산업분야의 적용가능성을 고찰하고자 하였다.

Chapter 1 Introduction

1.1 Research Background and Purpose

The biggest key technology in the various industry field of modern society will be "eco-friendly green growth" due to the atmospheric pollution, global warming and resource depletion in the world. To meet the need for energy reduction and protection of the environment, the various industry field of modern society are focussing on the green technology which have application to the decrease in thickness of material and use of lightweight material. Moreover, different types of household appliances with development of the global economic have been released in order to improve the quality and convenience of life. And an electric washing machine, one of the white goods, has been developed rapidly.

Stainless steel has been applied as high strength-to-weight ratio material for automobiles, aircraft and other machines. Ferritic stainless steel has good corrosion resistance, is used in demand-based industries including automobile and electrical appliance to meet the demand where considers the weight lightening and energy saving. Ferritic stainless steel has many advantages. Firstly, ferritic stainless steel are more economic because they do not contain nickel which is an expensive alloy¹⁾. And STS430J1L has become good a sight better weldability with Cu and Nb.

However, there are several problems in fusion welding of ferritic stainless steel. One of the problem is about excessive grain growth. It is possible to have the problem of coarse grains in weld zone and heat-affected zone. Also the coarse causes the low toughness and ductility²⁾. Another problem in the fusion welding of ferritic stainless steel is thermal deformation, residual stress and weld defects. In addition to

problem of ferritic stainless steel, another problem in fusion welding is formation of sigma-phase (σ -phase). Several undesirable intermetallic phases such as σ -phase may occur when stainless steels are exposed to 650–850°C for a period of time. The σ -phase is the most serious of these secondary phases due to its impact on the mechanical properties³⁾. To prevent the σ -phase, ferritic stainless steel must not be preheated over 400°C. Another solution is after welding stainless steel must be cooled very quick⁴⁾. But these problems can be avoided by using lower welding heat inputs.

To solve this problem, Friction Stir Welding (FSW) is a new solid state joining process which is invented by The Welding Institute of the United Kingdom (TWI) in 1981. Grain growth and weld defects in FSW can be avoided because the maximum temperature is lower than the melting point in comparison with fusion welding⁵⁾.

Various research works has already been reported about the application of FSW process. On friction stir welded (FSWeld) AISI 430 FSS in which about 95% property of the base metal was achieved⁶⁾. In a similar trend, weldability of FSS which was due to the presence of very fine duplex structure of ferrite and martensite in the weld microstructure formed consequent⁷⁾. And Meran and Canyurt searched the effect of tool rotation speed and traverse speed on welding of AISI 304 austenitic stainless steels by FSW method. They obtained the optimal strength with rotational speed of 950rpm and 47.5mm/min⁸⁾.

In this study, it was intended to investigate the weldability and mechanical characteristics of thin ferritic stainless steel by using FSW. Due to thin plate welding, tool of non-probe type is used in this study. Its other merit is that frictional heat occur under the shoulder in this thin butt joints and frictional heat passes throughout inside. Also butt joints has become grain refinement affecting dynamic recrystallization of strong

shearing deformation and frictional heat. Successfully obtaining the process of the experimental data will influence the industrial and national competitiveness.

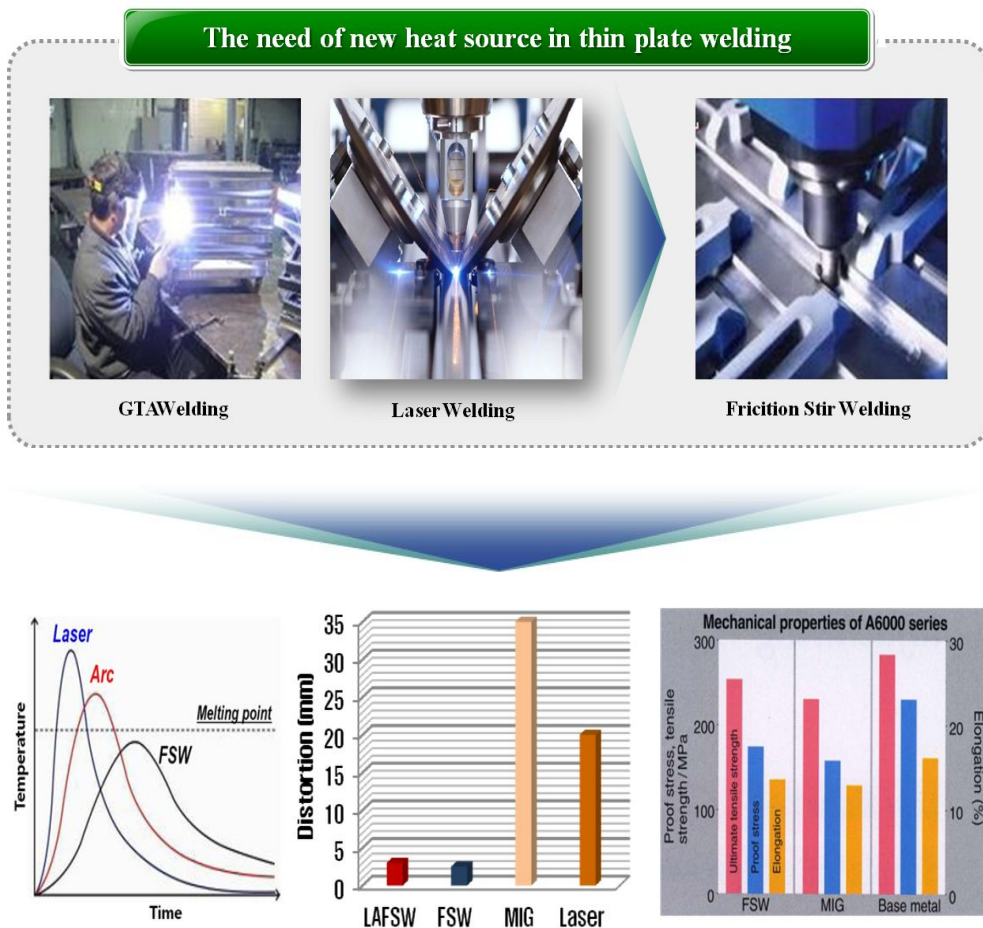


Fig. 1.1 Application of FSW to stainless steel

1.1.1 Application of FSW

Friction Stir Welding has been applied for automotive, rail, marine, aerospace, land transport and other machines. In the case of marine industry, FSW is used in panel for deck, Al extrusions and helicopter landing platform. In advanced country cases, university of adelaide was developed FSW moving system to build a light alloy cruise ships. Also Sweden and Norway of north europe apply for building a light alloy ships. These FSW technology obtain approval to apply for build from the classification ship's class(DNV, RINA, Lloyds). FSW technology is presently followed in a national shipbuilding industry.

In the case of automotive, Aluminium engine cradles and suspension struts for stretched Lincoln Town Car were the first automotive parts that were friction stir at Tower Automotive, who use the process also for the engine tunnel of the Ford GT. In Japan FSW is applied to suspension struts at Showa Denko and for joining of aluminium sheets to galvanized steel brackets for the boot (trunk) lid of the Mazda MX-5. Friction stir spot welding is successfully used for the bonnet (hood) and rear doors of the Mazda RX-8 and the boot lid of the Toyota Prius.

Also, boeing applies FSW to the Delta II and Delta IV expendable launch vehicles, and the first of these with a friction stir welded Interstage module was launched in 1999. The process is also used for the Space Shuttle external tank, for Ares I and for the Orion Crew Vehicle test article at NASA[dated info] as well as Falcon 1 and Falcon 9 rockets at SpaceX. The toe nails for ramp of Boeing C-17 Globemaster III cargo aircraft by Advanced Joining Technologies and the cargo barrier beams for the Boeing 747 Large Cargo Freighter were the first commercially produced aircraft parts. FAA approved wings and fuselage panels of the Eclipse 500 aircraft were made at Eclipse Aviation.

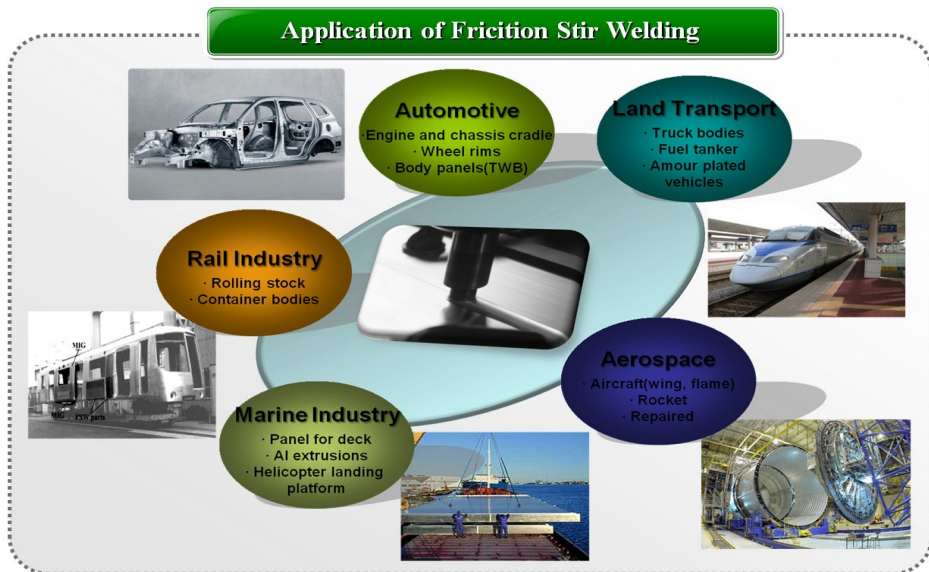


Fig. 1.2 Application of FSW in industries

1.1.2 Application of stainless steel in industries

While the original form of stainless steel, (iron with around 12% chromium) is still in widespread use, engineers now have a wide choice of different type(grades). In all, there are more than 100 different grades but these are usually sub-classified into distinct metallurgical "families" such as the austenitic, ferritic, martensitic and duplex families.

Although austenitic stainless steel has common use, ferritic stainless steel has many advantages. Firstly, ferritic stainless steels are more economic because they do not contain nickel which is an expensive alloy.

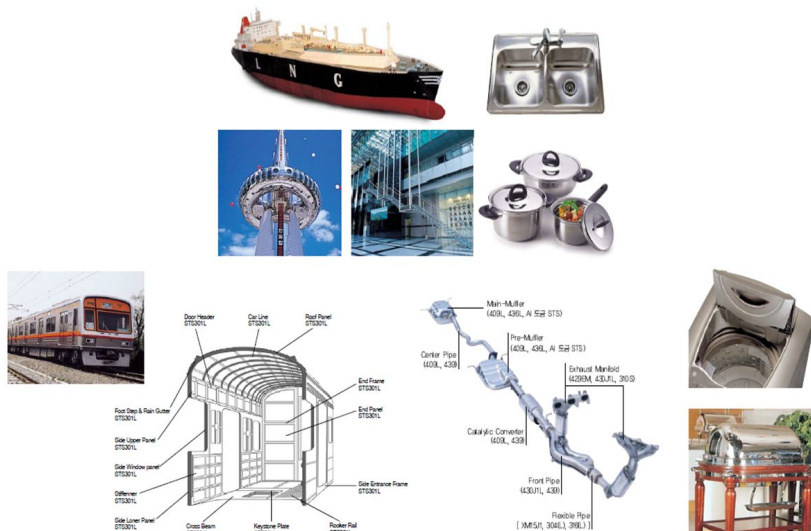


Fig. 1.3 Application of stainless steel in industries

1.2 Research Methodology

The methodology of this study is as in the following.

- 1) Experimental design on FSW
 - Design and fabrication of optimal jig
 - Design and fabrication of FSW tool
- 2) To find optimum welding conditions on FSW experiment
 - Tilt angle(°)
 - Rotation speed(rpm)
 - Travel speed(mm/min)
 - Dwell time(s)
 - Weld length(mm)
 - Back-up plate
 - Evaluation of bead on plate
- 3) Mechanical tests and microstructural analysis
 - Tensile test
 - Hardness test
 - Optical Microscope
 - Scanning Electron Microscope
- 4) Temperature history test
 - Thermocouple test

Chapter 2 Theoretical Background

2.1 Principle and Characteristics of FSW

2.1.1 Principle of FSW

Friction Stir Welding(FSW) is a solid-state joining process (the metal is not melted) and is used when the original metal characteristics must remain unchanged as much possible. It mechanically intermixes the two pieces of metal at the place of the join, then softens them so the metal can be fused using mechanical pressure, much like joining clay, dough or plasticine. A constantly rotated cylindrical shouldered tool with a profiled nib is transversely fed at a constant rate into a butt joint between two clamped pieces of butted material. The nib is slightly shorter than the weld depth required, with the tool shoulder riding atop the work surface.

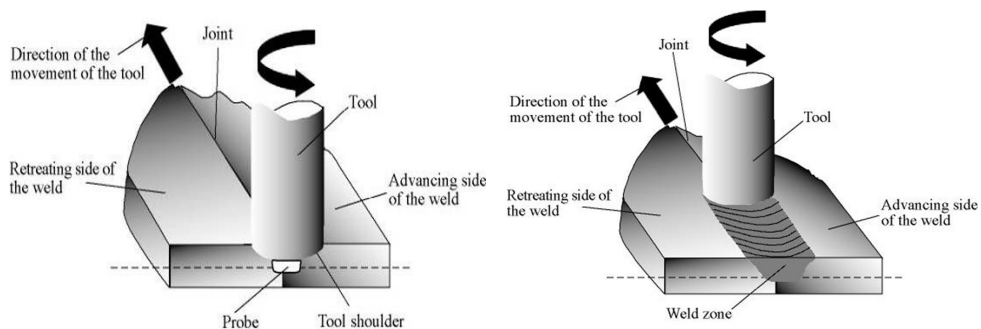


Fig. 2.1 Schematic diagram of FSW

Frictional heat is generated between the wear-resistant welding components and the work pieces. This heat, along with that generated by the mechanical mixing process and the adiabatic heat within the material,

cause the stirred materials to soften without melting. As the pin is moved forward, a special profile on its leading face forces plasticised material to the rear where clamping force assists in a forged consolidation of the weld.

This process of the tool traversing along the weld line in a plasticised tubular shaft of metal results in severe solid state deformation involving dynamic recrystallization of the base material.

2.1.2 Characteristic microstructure of FSW

The solid-state nature of the FSW process, combined with its unusual tool and asymmetric nature, results in a characteristic microstructure. The microstructure can be broken up into the following zone :

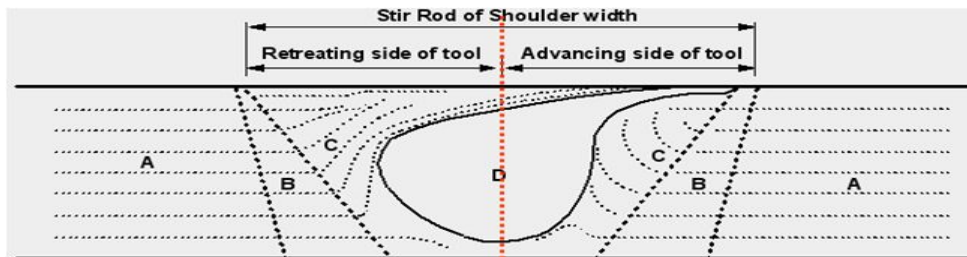


Fig. 2.2 Microstructural regions of Friction Stir Welding

A : The base metal (BM) is no change.

The heat-affected zone (HAZ) is common to all welding processes. As indicated by the name, this region is subjected to a thermal cycle but is not deformed during welding. The

B : temperatures are lower than those in the TMAZ but may still have a significant effect if the microstructure is thermally unstable. In fact, in age-hardened aluminium alloys this region commonly exhibits the poorest mechanical properties.

The thermo-mechanically affected zone (TMAZ) occurs on either side of the stir zone. In this region the strain and temperature

C : are lower and the effect of welding on the microsturcture is correspondingly smaller. Unlike the stir zone the microstructure is recognizably that of the parent material, albeit significantly

deformed and rotated. Although the term TMAZ technically refers to the entire deformed region it is often used to describe any region not already covered by the terms stir zone and flow arm.

D : The stir zone (also nugget, dynamically recrystallised zone) is a region of heavily deformed material that roughly corresponds to the location of the pin during welding. The grains within the stir zone are roughly equiaxed and often an order of magnitude smaller than the grains in the parent material. A unique feature of the stir zone is the common occurrence of several concentric rings which has been referred to as an "onion-ring" structure. The precise origin of these rings has not been firmly established, although variations in particle number density, grain size and texture have all been suggested.

2.1.3 Generation and flow of heat

Heating generation during friction stir welding arises from two source : friction at the surface of the tool and the deformation of the material around the tool. The heat generation is often assumed to occur predominantly under the shoulder, due to its greater surface area, and to be equal to the power required to overcome the contact forces between the tool and the workpiece. The contact condition under the shoulder can be described by sliding friction, using a friction coefficient μ and interfacial pressure P , or sticking friction, based on the interfacial shear strength at an appropriate temperature and strain rate. Mathematical approximations for the total heat generated by the tool shoulder Q_{total} have been developed using both sliding and sticking friction model :

$$Q_{total} = \frac{2}{3}\pi P\mu\omega(R_{shoulder}^3 - R_{pin}^3)(Sliding)$$

$$Q_{total} = \frac{2}{3}\pi\tau\omega(R_{shoulder}^3 - R_{pin}^3)(Sticking)$$

where ω is the angular velocity of the tool, $R_{shoulder}$ is the radius of the tool shoulder and R_{pin} that of the pin. Several other equations have been proposed to account for factors such as the pin but the general approach remains the same. A major difficulty in applying these equations is determining suitable values for the friction coefficient or the interfacial shear stress. The conditions under the tool are both extreme and very difficult to measure. To date, these parameters have been used as fitting parameters where the model works back from measured thermal data to obtain a simulated thermal field. While this approach is useful for creating process models to predict, for example, residual stresses it is less useful for providing insights into the process itself.

2.1.4 Advantages and limitations of FSW

The solid-state nature of FSW leads to several advantages over fusion welding methods as problems associated with cooling from the liquid phase are avoided. Issues such as porosity, solute redistribution, solidification cracking and liquation cracking do not arise during FSW. In general, FSW has been found to produce a low concentration of defects and is very tolerant of variations in parameters and materials.

1) Advantages of Friction Stir Welding

- Good mechanical properties in the as-welded condition.
- Improved safety due to the absence of toxic fumes or the spatter of molten material
- No consumables
- Easily automated on simple milling machines—lower setup costs and less training.
- Can operate in all position(horizontal, vertical, etc.), as there is no weld pool.
- Generally good weld appearance and minimal thickness under/over-matching, thus reducing the need for expensive machining after welding.
- Low environmental impact.

2) Limitations of Friction Stir Welding

- Exit hole left when tool is withdrawn.

- . Large down forces required with heavy-duty clamping necessary to hold the plates together.
- . Less flexible than manual and arc processes (difficulties with thickness variations and non linear welds).
- . Often slower traverse rate than some fusion welding techniques, although this may be offset if fewer welding passes are required.

2.2 Classification of stainless steel

The worldwide consumption of stainless steel is increasing. There is growing demand from the building and construction industry where stainless steel is used for its attractive appearance, corrosion resistance, low maintenance and strength. Many other industries are adopting stainless steel for similar reasons as well as the fact that it does not need to be treated, coated or painted when put into service, despite the fact that it is more expensive than plain carbon steels.

1) Ferritic Stainless Steels

These are plain chromium (10.5 to 18%) grades such as Grade 430 and 409. Their moderate corrosion resistance and poor fabrication properties are improved in the higher alloyed grades such as Grades 434 and 444 and in the proprietary grade 3CR12. Although austenitic stainless steel has common use, ferritic stainless steel has many advantages.

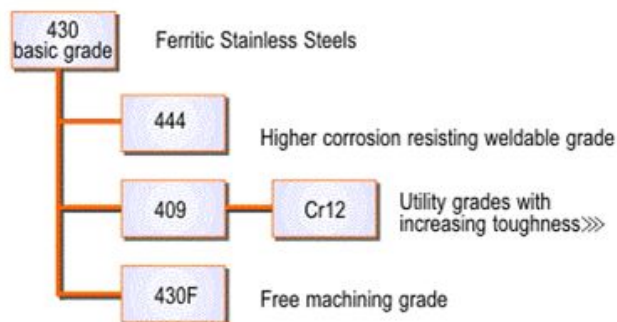


Fig. 2.3 Classification of ferritic stainless steels

2) Austenitic Stainless Steels

This group contains at least 16% and 6% nickel and range through to the high alloy super austenitics such as 904L and 6% molybdenum grades. Additional element can be added such as molybdenum, titanium or copper, to modify or improve their properties, making them suitable for many critical applications involving high temperature as well as corrosion resistance. This group of steels also suitable for cryogenic applications because the effect of the nickel content in making the steel austenitic avoids the problems of brittleness at low temperatures, which is a characteristic of other types of steel.

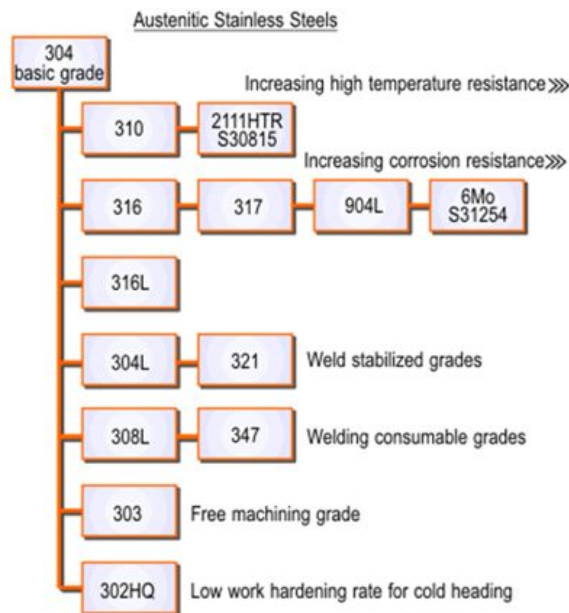


Fig. 2.4 Classification of austenitic stainless steels

3) Martensitic Stainless Steels

Martensitic stainless steels are also based on the addition of chromium as the major alloying element but with a higher carbon and generally lower chromium content than the ferritic types : Grade 431 has a chromium content of about 16%, but the microstructure is still martensite despite this high chromium level because this grade also contains 2% nickel.

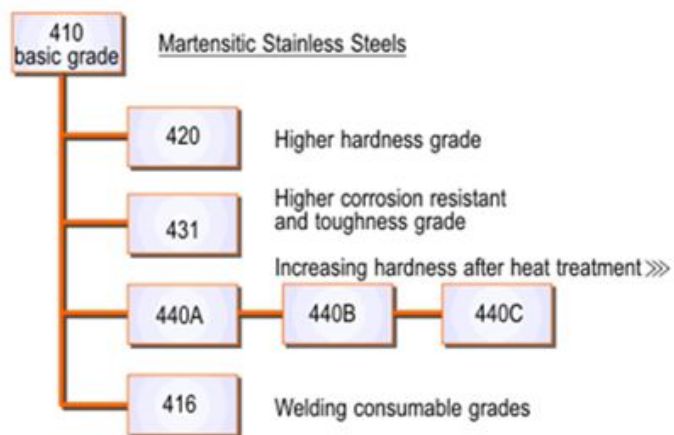


Fig. 2.5 Classification of martensitic stainless steels

Chapter 3 Experimental Method of Friction Stir Welding Process

3.1 Experimental Details

3.1.1 Experimental equipment

In order to carry out the FSW experiment, WINXEN FSW gantry type system is used in this thin plate welding experiment. And FSW machine is able to move the triaxis (X, Y, Z). Fig. 3.1 shows the specifications of WINXEN FSW gantry type system.

In comparison with existing FSW method, No probe of used tool is Other feature in this study. When shoulder of tool rotate on an axis, the frictional heat is generated on surface of metals. Tungsten carbide (WC-Co12%) tool having shoulder diameter of 6mm was used in the experiment.

The back-up plate is stainless steel 430J1L of the same quality because the frictional heat loss occur from the back plate. Also, The stainless steel have low heat conductivity and thermal expansion. A shoulder of rotating tool is forced to plunge into the plates to be welded and move along the central contact line.

Dwell time is that the material is preheated by a stationary, rotating tool to get a sufficient heat input. This period helps butt joints to increase heat generation. And so dwell time is very important variable in this study because the initial section of thin butt joints can't be welded due to the lack of frictional heat. Fig. 3.2 shows the experimental set-up for FSW of thin plate.

Fig. 3.1 Specifications of FSW system

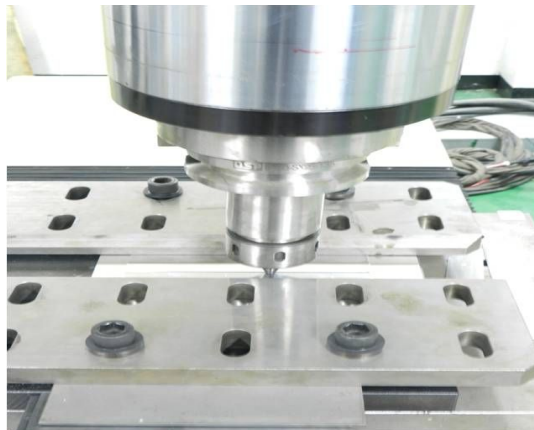


Fig. 3.2 Experimental set-up for FSW

3.1.2 Objective material

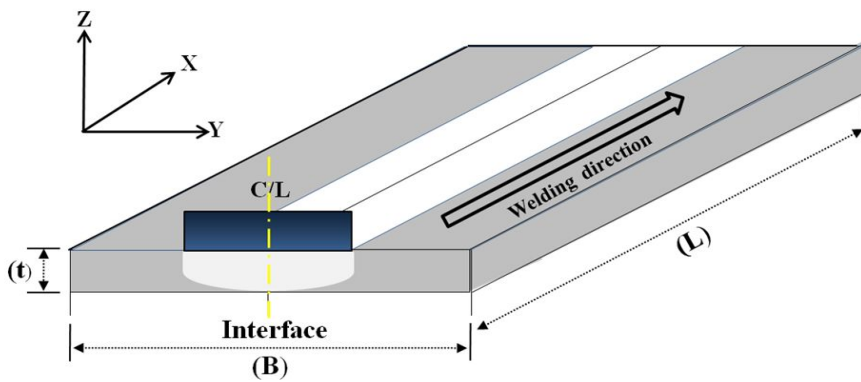
STS430J1L Stainless steel was used in this study. This stainless steel has a typical contents of 16.47Cr-0.286Nb-Low (C, N) in ferritic type which improved processing, anti-corrosion, heat-resistance and welding performance of STS430 significantly. It increased more chrome contents than STS430 and improved the anti-corrosion because STS430J1L has became good a sight better weldability with Cu and Nb.

The chemical compositions and mechanical properties of the materials are shown in Table 3.1. Two sheets with dimensions of 0.5(t)×160(B)×150(L) mm were joined in butt joints. To minimize the formation of burr, specimens of the contact side was done by milling process. The welding surface was wiped with Methyl Alcohol to remove the grease before welding process. Table. 3.2 shown the dimension of used specimen.

Table. 3.1 Chemical compositions and mechanical properties

Table. 3.2 Configuration of used specimen

Unit : mm			
Material	L	B	t
STS430JIL	150	160	0.5



3.1.3 Description of tool material and shape

The material of tool is made of 12%Co tungsten carbide (WF20) to prevent wear-resistant of tool due to frictional contact with stainless steel plates while conducting FSW process. The chemical compositions and mechanical properties of the used tool in this study are shown in Table. 3. 3.

No probe of used tool is Other feature in this study. When shoulder of tool rotate on an axis, the frictional heat is generated on interface of metals. Tungsten carbide (WC-Co12%) tool having shoulder diameter of 6mm was used in the experiment. Fig. 3.3 shows the dimension and shape of tool.

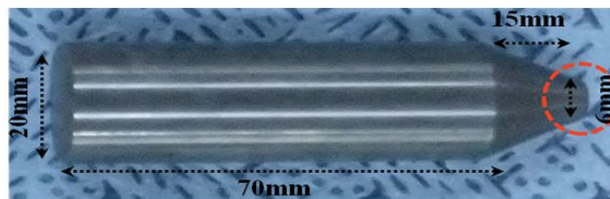
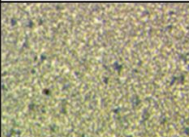


Fig. 3.3 Dimension and shape of tool

Table. 3.3 Chemical compositions and mechanical properties of tool

Material : WC-12wt%Co						
Co ($\pm 0.5\%$)	Grade	WC ($\pm 0.5\%$)	Grain Size (μm)	Density (g/cm^3)	Hardness (HV30)	Microstructure
12%	WF20	88%	0.6	14.15	1670	

3.2 Experimental procedure

To carry out the FSW experiment for thin plate welding, First of all, key process variables were established during the FSW. In the case of back-up plate, stainless steel 430J1L of the same quality was used to minimize the heat loss from the back plate. And tilt angle were kept fixed (2°).

Secondly, rotation speed and travel speed are variable. Rotation speeds were chosen at 800, 850, 900rpm and travel speeds were 84, 96, 108mm/min. As a result of experiment, a cross section of the joint were not welded at rotation speed below 800rpm. Welding parameters are shown in Table. 3.4.

Thirdly, after the FSW had been finished, mechanical test of joints was carry out to get the tensile strength. cross-head speed of Tensile test was 0.0333mm/sec to comply with the korean standard (KS B 0801 13-B). Also, hardness test was carry out by vickers tester.

Fourthly, after the FSW had been finished, visual inspection of joints was examined to check the defects on the bead surface and then metallurgical examination were done after polishing and etching.

Table. 3.4 Welding parameters of FSW

Welding parameter		Values
FSW	Rotation speed (rpm)	700, 800, 900
	Welding speed (mm/min)	84 , 96, 108
	Dwell time (S)	15
	Tilt angle (°)	3
	Room temperature(°C)	21
	Shoulder size (mm)	Ø6
	Weld length (mm)	130
	Back-up plate	STS430J1L

3.3 Mechanical Evaluation

3.3.1 Tensile test

Fundamentally, the process involves placing the test specimen in the testing machine and applying tension to it until it fractures. During the application of tension, the elongation of the gauge section is recorded against the applied force. The data is manipulated so that it is not specific to the geometry of the test sample. The elongation measurement is used to calculate engineering strain, ε , using the following equation :

$$\varepsilon = \frac{\Delta L}{L_0} = \frac{L - L_0}{L_0}$$

where ΔL is the change in gauge length, L_0 is the initial gauge length, and L is the final length. The force measurement is used to calculate the engineering stress, σ , using the following equation :

$$\sigma = \frac{F_n}{A}$$

where F is the force and A is the cross-section of gauge section. The machine does these calculations as the force increases, so that data points can be graphed into a stress-strain curve.

Tensile test was carried out with Dongil-Simaz Universal Testing Machine (EHF-EG200KN-40L) using WINSERVO program. Fig. 3.4 shows the EHF-EG200KN-40L and tensile testing setup.

The specimens are fabricated in accordance with the korean standards (KS B 0801 13-B). The specimen dimensions are given in Table 3.5. Tensile test was done with Load speed 0.0333mm/sec and stress-strain curve was obtained.

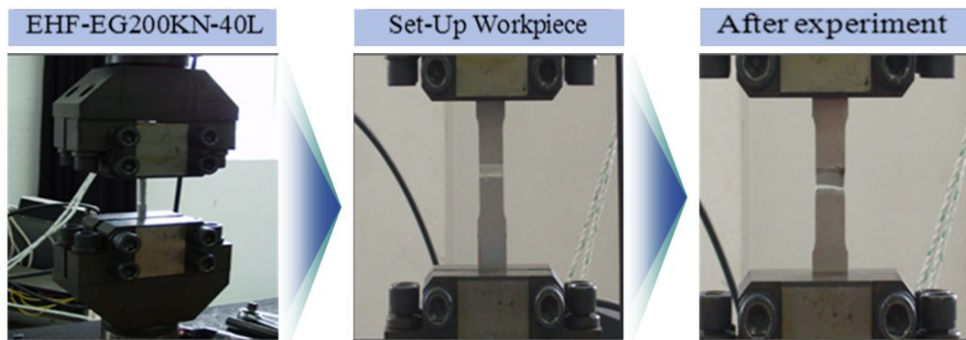
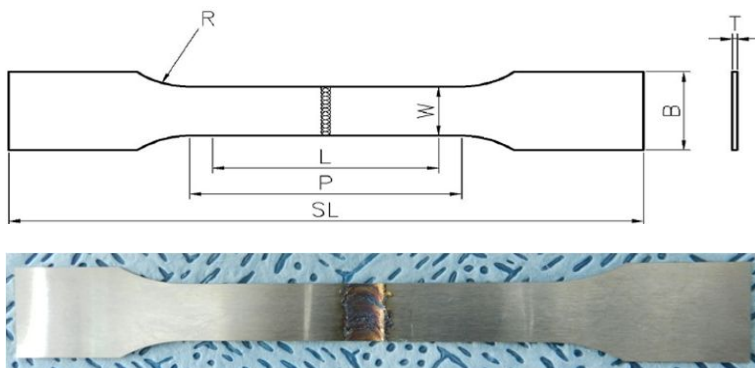


Fig. 3.4 Tensile test machine

Table. 3.5 Geometry of tensile test specimen



W	L	P	R	T	B	SL
12.5mm	50mm	60mm	20mm	0.5mm	20mm	120mm
KS B 0801 13B						

- L : Gauge length
- P : Length of reduced section
- T : Thickness
- R : Radius of fillet
- B : Width of grip section
- W: Width
- SL : Over-all length

3.3.2 Hardness test

Generally, loads of various magnitudes are applied to a flat surface, depending on the hardness of the material to be measured. The HV number is then determined by the ratio F/A where F is the force applied to the diamond in kilograms-force and A is the surface area of the resulting indentation in square millimeters. A can be determined by the formula

$$A = \frac{d^2}{2\sin(136^\circ/2)}$$

which can be approximated by evaluating the sine term to give

$$A \approx \frac{d^2}{1.8544}$$

where d is the average length of the diagonal left by the indenter in millimeters. Hence,

$$HV = \frac{F}{A} \approx \frac{1.8544F}{d^2}$$

where F is in kgf and d is in millimeters. The corresponding units of HV are then kilograms-force per square millimeter (kgf/mm²). To calculate Vickers hardness number using SI units one needs to convert the force applied from kilogram-force to newtons by multiplying by 9.80665 (standard gravity) and convert mm to m. To do the calculation directly, the following equation can be used :

$$HV = \frac{F}{A} \approx \frac{0.1891F}{d^2}$$

where F is newton and d is millimeters.

The hardness of welded specimen was measured using Akashi HM-112 Vickers Hardness tester as shown in Fig. 3.5 and 3.6. The indenter employed in the Vickers test was a square-based pyramid whose opposite sides meet at the apex at an angle of 136° with load 500g applied for 10 sec. Fig. 3.6 shows hardness measurement points of welded specimen.

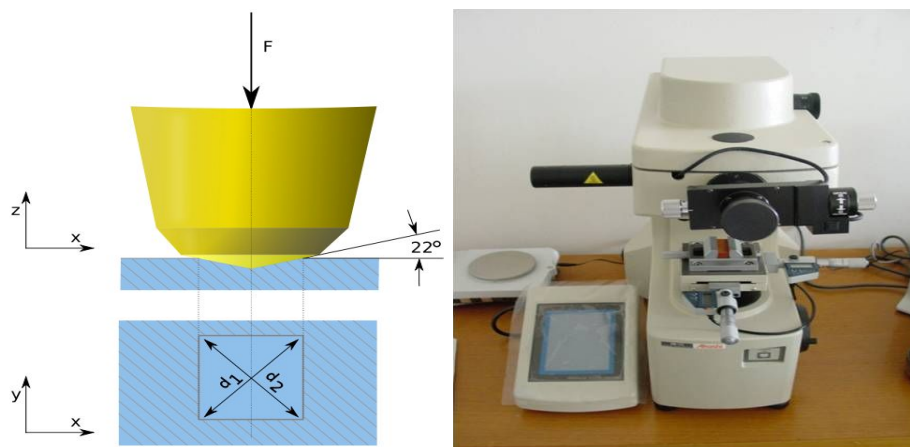


Fig. 3.5 Vickers hardness test scheme and machine

Table. 3.6 Hardness testing condition

	Values
Type	Micro vickers hardness tester
Load	0.5kgf
Loading time	10 sec.
Test position	Bellow 0.25mm on surface

3.4 Metallurgical Evaluation

The metallurgical investigations on a cross section of the joint were done after polishing and etching. The cross section of FSWelded butt joints was cut perpendicular to the welding direction. It was polished with 9, 3 and 1 μ m diamond paste, and then the specimen was chemically etched in a "Aqua ria"(20ml HNO₃ +60ml HCl) for a period of 10 seconds to observe the macro and microstructure. Fig. 3.7 shows the optical microscope.



Fig. 3.6 Optical microscope

The types of signals produced by a SEM include secondary electrons (SE), back-scattered electrons (BSE), characteristic X-rays, light (cathodoluminescence) (CL), specimen current and transmitted electrons.

Secondary electron detectors are standard equipment in all SEMs, but it is rare that a single machine would have detectors for all possible signals. The signals result from interactions of the electron beam with atoms at or near the surface of the sample. In the most common or standard detection mode, secondary electron imaging or SEI, the SEM can produce very high-resolution images of a sample surface, revealing details less than 1 nm in size. Due to the very narrow electron beam, SEM micrographs have a large depth of field yielding a characteristic three-dimensional appearance useful for understanding the surface structure of a sample. This is exemplified by the micrograph of pollen shown above. A wide range of magnifications is possible, from about 10 times (about equivalent to that of a powerful hand-lens) to more than 500,000 times, about 250 times the magnification limit of the best light microscopes.

3.5 Temperature Measurement

A thermocouple is a sensor for measuring temperature. It consists of two dissimilar metals, joined together at one end. When the junction of the two metals is heated or cooled a voltage is produced that can be correlated back to the temperature. The thermocouple alloys are commonly available as wire. And a thermocouple is available in different combinations of metals or calibrations. The four most common calibrations are J, K, T and E. The Fig. 3.8 shows the common thermocouple temperature ranges.

The temperature gradient at mid thickness were measured at six point locations during the FSW process using MIDI LOGGER GL220-UM-851 and thermocouples (K type) which placed diameter inserted into approximately 0.3mm diameter holes drilled on top side of specimens. K type was chosen in this study because K type was economical and proper.

Common Thermocouple Temperature Ranges			
Calibration	Temp Range	Std. Limits of Error	Spec. Limits of Error
J	0°C to 750°C (32°F to 1382°F)	Greater of 2.2°C or 0.75%	Greater of 1.1°C or 0.4%
K	-200°C to 1250°C (-328°F to 2282°F)	Greater of 2.2°C or 0.75%	Greater of 1.1°C or 0.4%
E	-200°C to 900°C (-328°F to 1652°F)	Greater of 1.7°C or 0.5%	Greater of 1.0°C or 0.4%
T	-250°C to 350°C (-328°F to 662°F)	Greater of 1.0°C or 0.75%	Greater of 0.5°C or 0.4%

Fig. 3.7 Common thermocouple temperature ranges

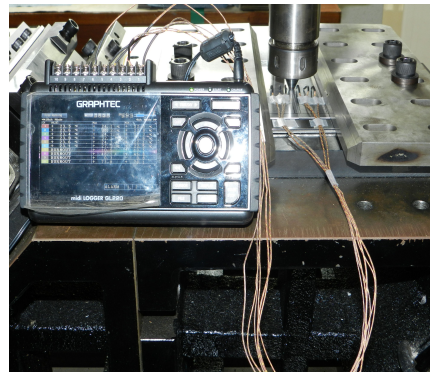
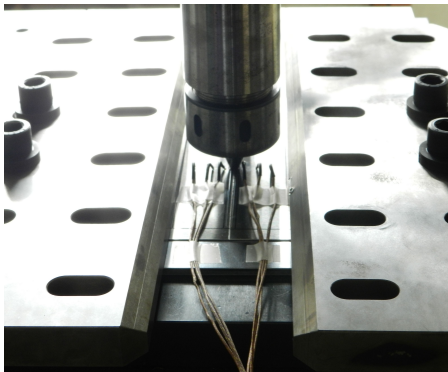


Fig. 3.8 Set-up for temperature measurement

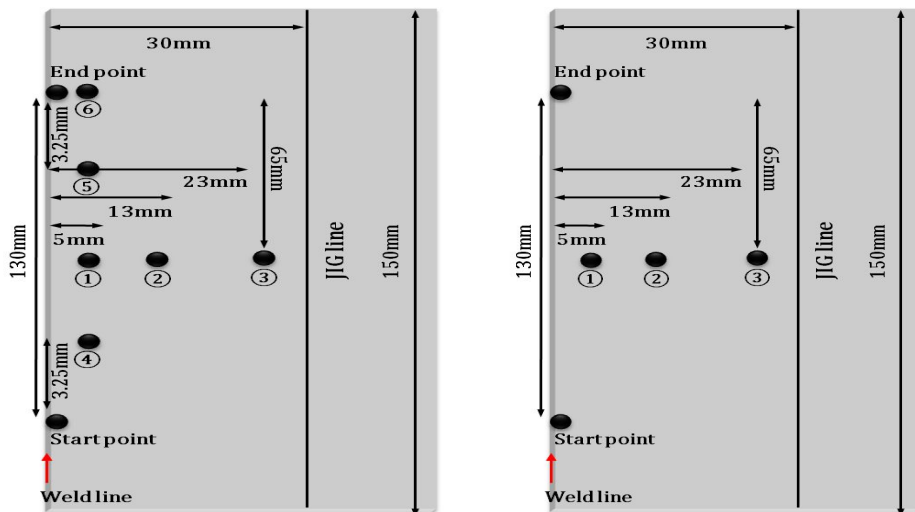


















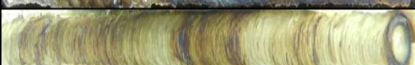

Fig. 3.9 Thermocouple positions on workpiece

Chapter 4 Results and Discussions

4.1. Bead Profiles

Table 4.1 shows the bead appearance and cross section of FSW welds with travel speed of 84, 96, 108mm/min in different rotation speeds of 800, 850, 900rpm. It was observed that defects occurred on the surface and cross section of joints at a tool rotation speed of 800, 850rpm and travel speed of 84, 96, 108mm/min. However, the width of the plastically deformed region was observed at a tool rotation speed of 900rpm and travel speed of 84, 96, 108mm/min. Distinctively, the width of the plastically deformed region decreased down the vertical direction.

Table. 4.1 Bead profiles of welds for various travel speed in different rotation speed

RPM	Travel Speed (mm/min)	Bead Appearance	Cross Section (Macro)
800	84		
	96		
	108		
850	84		
	96		
	108		
900	84		
	96		
	108		

4.2. Mechanical Characteristics

4.2.1 Tensile strength

Fig. 4.1. shows the tensile test welded specimens obtained from different travel speeds with travel speed of 84~108mm/min in tool rotation speed of 900rpm. Fig. 4.2 shows the comparison of tensile strength of welds fabricated under above welding conditions. From the results, it was found that maximum tensile strength of welds was 450MPa under travel speed of 96mm/min. The tensile strength of the 84mm/min joints was 430MPa and the tensile strength of 108mm/min joints was 388MPa, respectively. The maximum tensile strength of 96mm/min was approximately 97% in comparison with that of base metal. Table 4.3 and Fig 4.3 show fractured specimens and stress-strain curves of FSW welds at 900rpm with different travel speeds.

Moreover, tensile strength of end part of FSW welds, which regarded as the weld defect was investigated. It was observed that end part of FSW welds of thin plate indicated the good tensile strength which was 488MPa. It can be inferred that because of increasement of heat input by dwell time at end part. Fig 4.4 shows the stress-strain curve of end part of FSW welds.

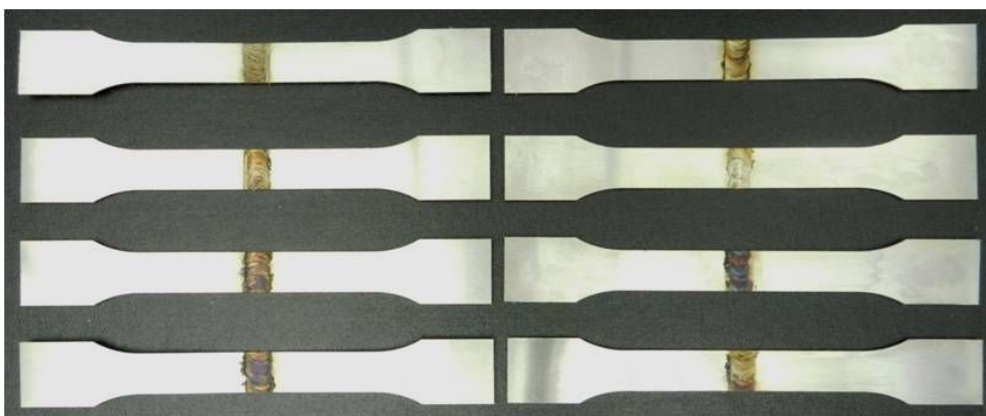


Fig. 4.1 Tensile test specimens

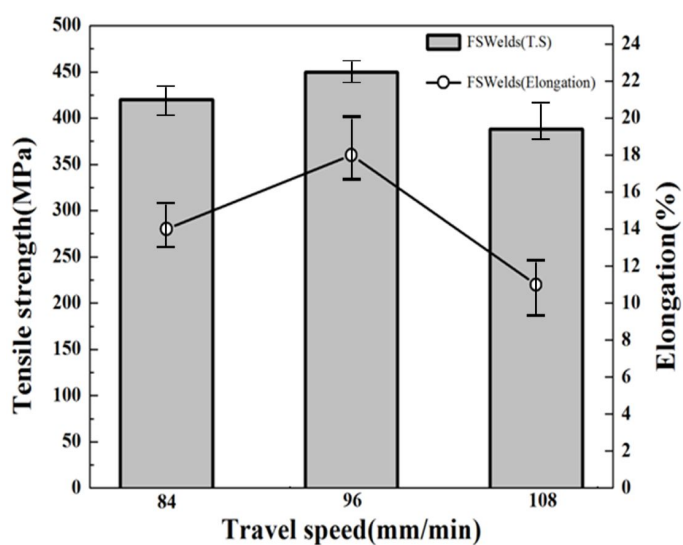





Fig. 4.2 Comparison of tensile strength of FSW welds with travel speed

Table. 4.2 Tensile strength and fractured specimen after tensile test for various travel speed in different rotation speed

RPM	Travel Speed (mm/min)	Fractured Specimens	Tensile Stress (MPa)
800	84	-	-
	96	-	-
	108	-	-
850	84	-	-
	96	-	-
	108	-	-
900	84		430
	96		450
	108		388

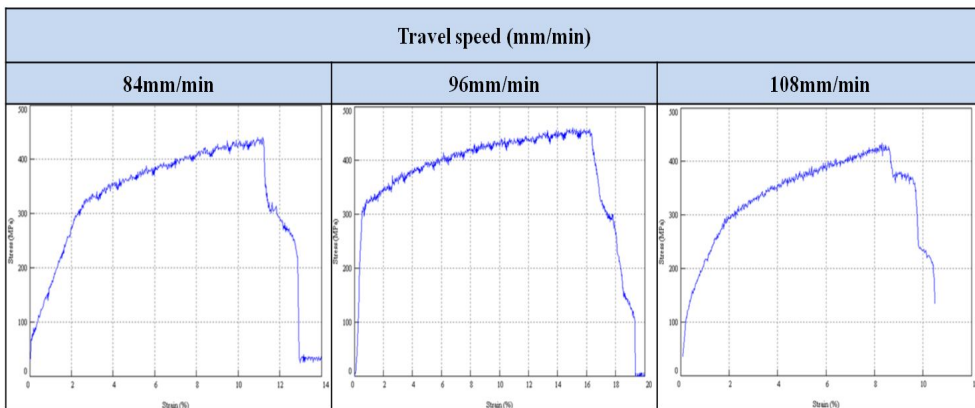


Fig. 4.3 Comparison of stress-strain curves of FSW welds with travel speed

**Result of tensile test of end part
(900rpm_96mm/min)**

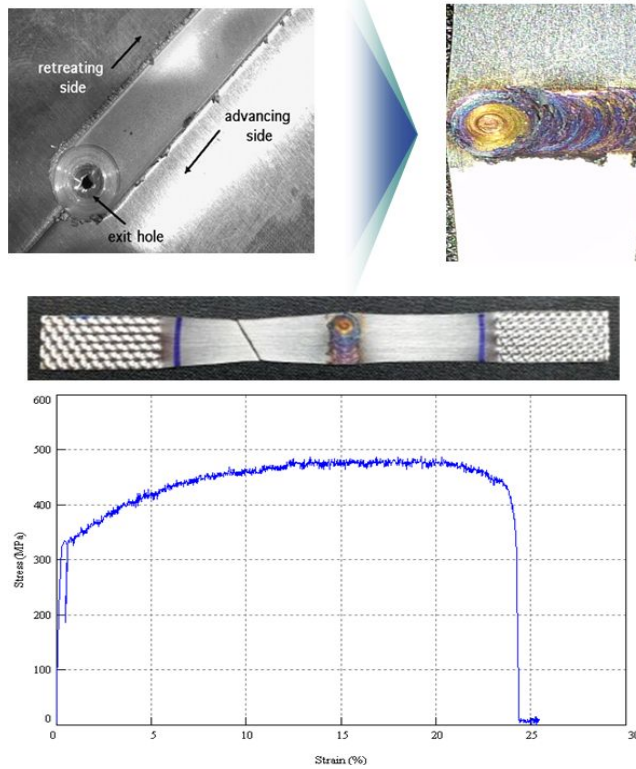


Fig. 4.4 Stress-strain curve for end part of FSW welded specimen

4.2.2 Hardness

Fig 4.5 shows the hardness distributions of welds in transverse direction of welding cross section at the distance 0.25mm away from top surface. The hardness at welds was higher than that of base metal which is due to the strong shearing deformation and frictional heat affecting dynamic recrystallization. The hardness of interface between base metal and joints was higher than that of base metal. It is thought that the regions of these hardness distributions probably corresponds to heat affected zone (HAZ) or thermo-mechanically affected zone (TMAZ). The other reason of increasing hardness is formation of martensite of welds. It was found that maximum hardness occurred in stir zone (SZ) and was approximately 275 Hv.

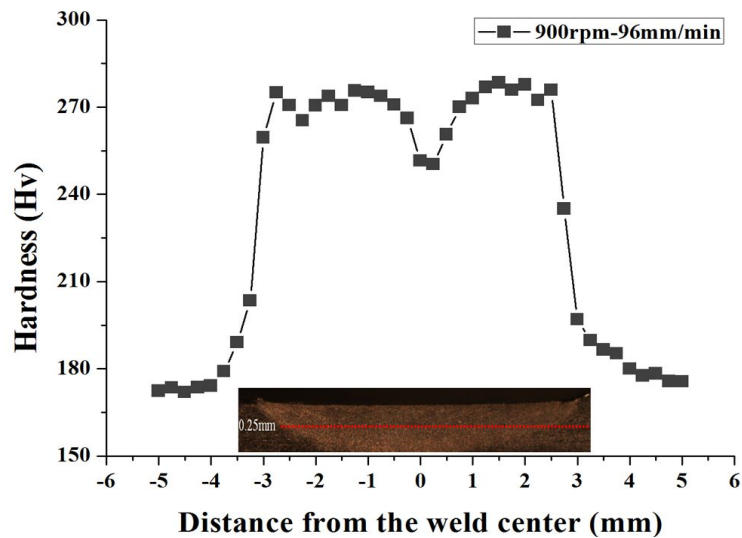


Fig. 4.5 Hardness distributions of FSW welds

4.3 Metallurgical Characteristics

Fig. 4.6 shows the microstructure (OM) of FSWelded joints at tool rotation speed of 900rpm and travel speed of 96mm/min. This microstructure is split into four groups, point A, B, C and D. However, there is little difference between the point A and B. The point A is retreating side and point D is advancing side. The slightly finer recrystallized grains in the joints (point C) are attributed to the generation of strong shearing deformation and frictional heat affecting dynamic recrystallization.

This microstructure has a clear characteristic to optical microscope images in the way that it is hard to tell the heat affected zone (HAZ) and thermo-mechanically affected zone (TMAZ) respectively.

The width of the plastically deformed region decreased to vertical direction because frictional heat occur under the shoulder in this thin butt joints and frictional heat passes throughout inside. In comparison with back-up plate used, the stainless steel 430J1L of the same quality is superior to the Al alloy or mild steel at the depth of the plastically deformed region.

Fig. 4.6 Optical microstructure of FSW welds

The grain sizes and elements of butt joints were examined using a scanning electron microscope (SEM) equipped with an energy dispersive X-ray spectroscopy (EDS). Fig. 4.7 shows the SEM observation of microstructure at tool rotation speed of 900rpm and travel speed of 96mm/min. In comparison with grain size of butt joints, the grain sizes of base metal (point A) were approximately average $20\mu\text{m}$. However, the grain sizes of butt joints (point C) decreased to about $5\mu\text{m}$, because the slightly finer recrystallized grain in the joint are attributed to the

generation of strong shearing deformation and frictional heat affecting dynamic recrystallization. In the process of microstructure analysis (SEM), niobium of alloying element in joints has been observed. Niobium is a chemical element with the symbol Nb and atomic number 41 and paramagnetic metal in group 5 of the periodic table. It is a soft, grey, ductile transition metal. Although alloys contain only a maximum of 0.1%, that small percentage of niobium improves the strength of the steel.

The microstructure of the fractured specimens were analyzed after the tensile test. Fig. 4.8 shows the microstructure (SEM) of fractured specimens. The ductile fracture with dimple pattern and brittle fracture are observed in the specimens at travel speed of 84mm/min and 96mm/min, but brittle fracture is observed at 108mm/min. As a result of tensile fracture surface of end part at travel speed of 1.6mm/min, the ductile fracture with dimple is observed. Fig. 4.9 shows the SEM observation of fracture surface after tensile test in end part of butt joints at tool rotation speed of 900rpm and travel speed 96mm/min.

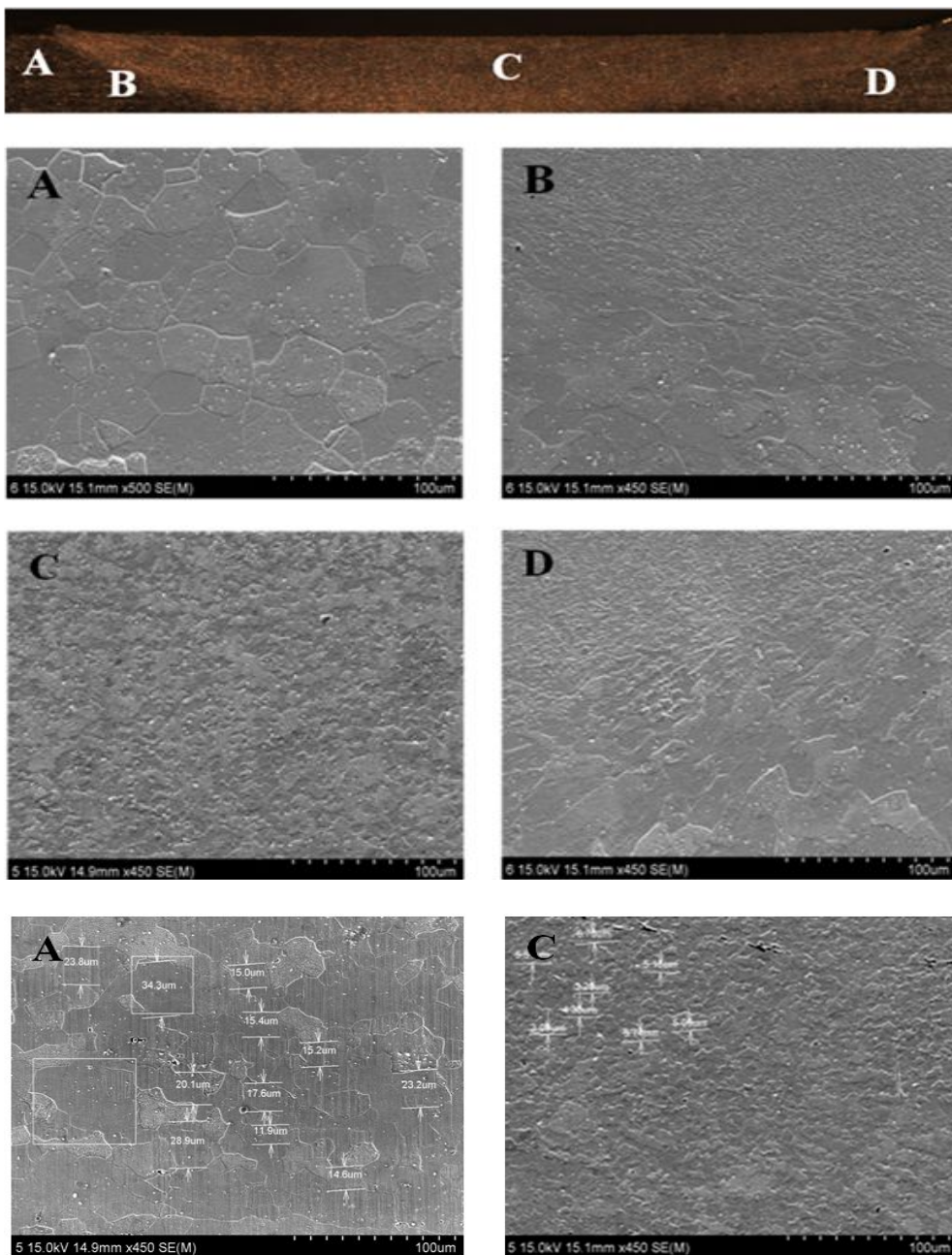
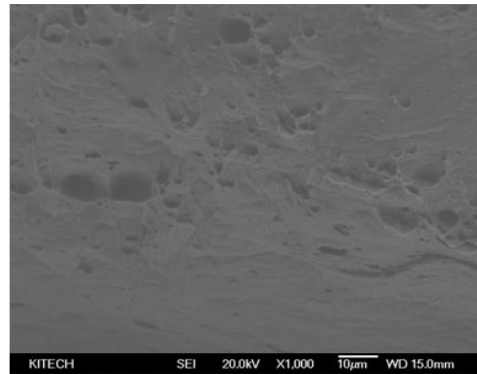
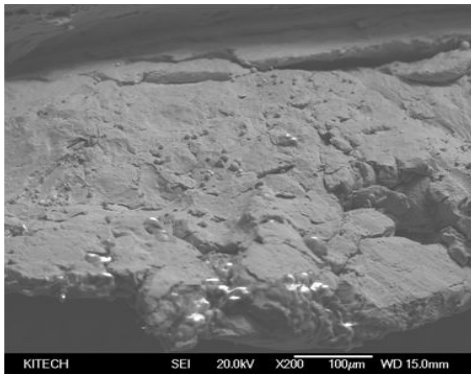
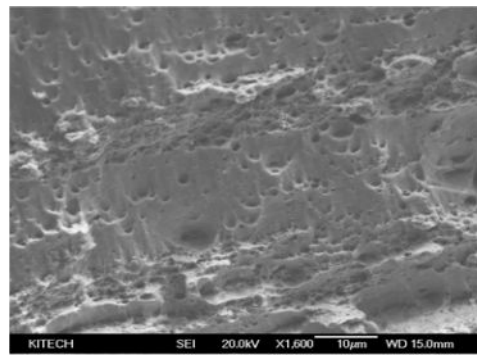
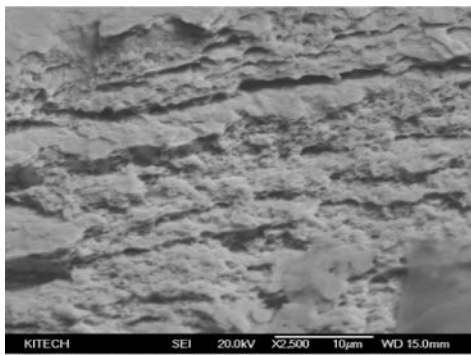


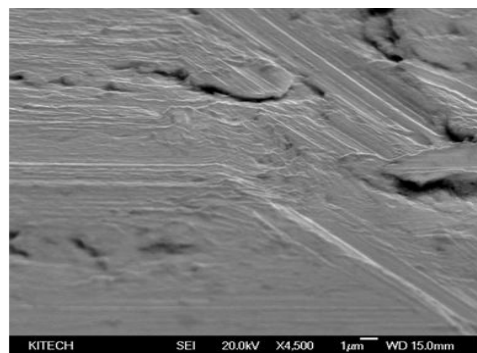
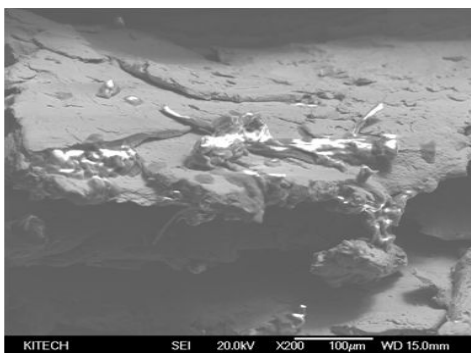
Fig. 4.7 SEM image of FSW welds



(a)84mm/min, 900rpm



(b)96mm/min, 900rpm



(c)108mm/min, 900rpm

Fig. 4.8 SEM observation of fracture surface after tensile test with travel speed

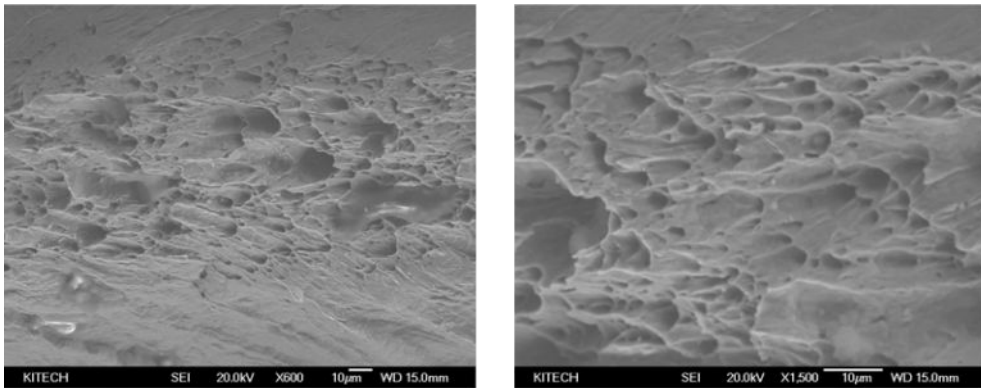


Fig. 4.9 SEM observation of fracture surface after tensile test for end part of welded specimen

4.5 Measured Temperature History

Fig. 4.10 shows the temperature history of FSW welds. As a result of temperature history, the temperature of start part is 109°C, which is lower than other points. This low temperature has caused poor weldability due to lack of frictional heat, but maximum temperature of end part has been measured to be 312°C, which improves tensile strength.

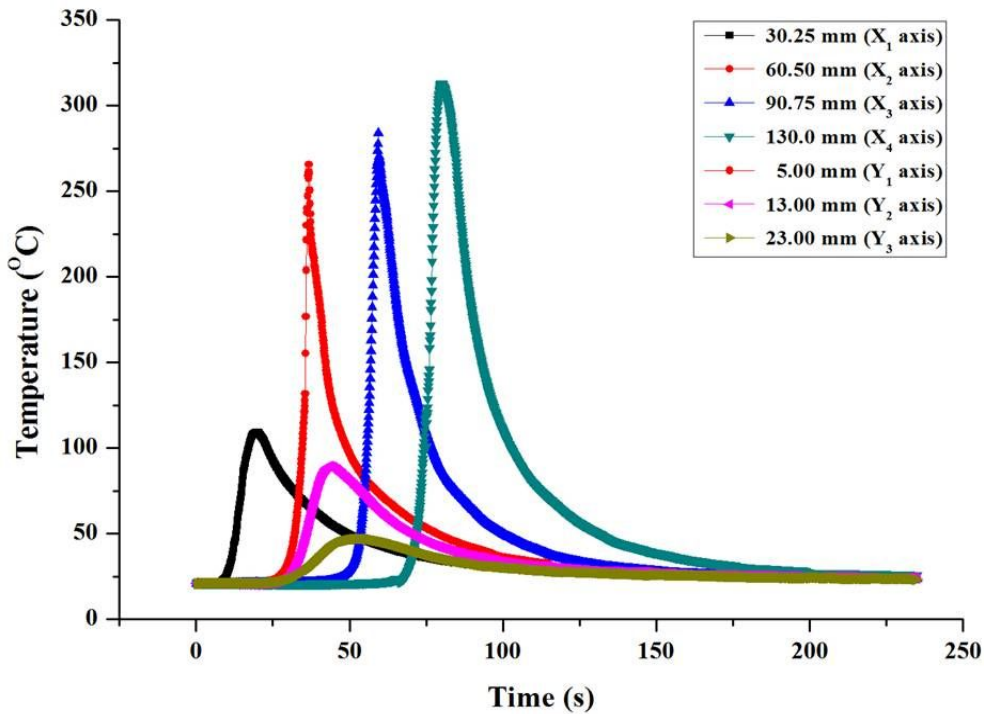


Fig. 4.10 Temperature history of FSW welds

Fig. 4.11 shows the comparison of temperature gradient of FSW welds and GTAW welds. As a result of temperature history, the temperature of FSW welds is lower than that of GTAW welds. Therefore, this temperature characteristics can be results in reduction of weld defects such as thermal deformation, residual stress etc.

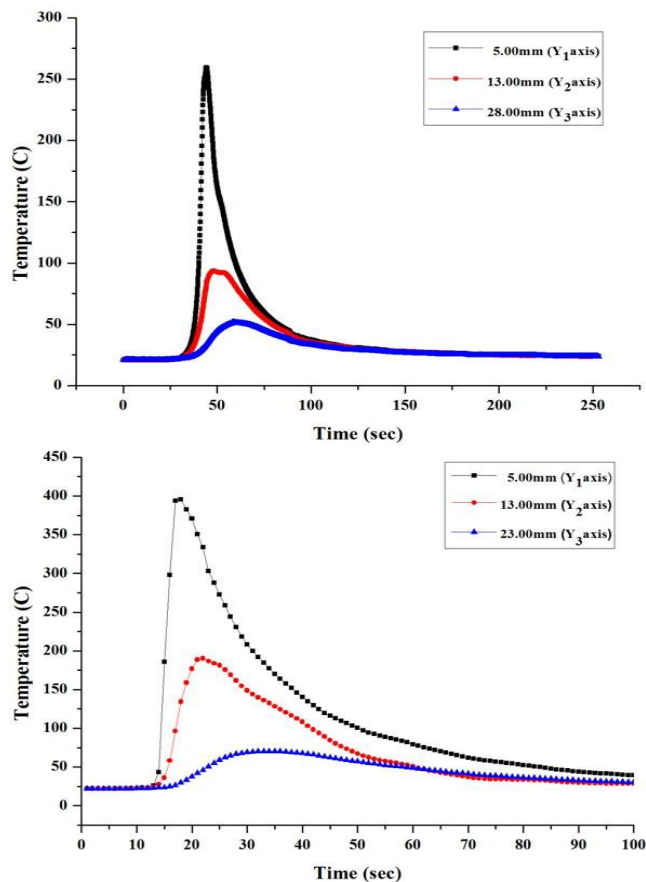


Fig. 4.11 Comparison of Temperature gradient of FSW welds and GTAW welds

Chapter 5 Conclusion

Friction Stir Weiding has great potential as a new welding technology. This study was intended to investigate the weldability, mechanical characteristics (tensile and hardness test) and microstructure analysis of thin ferritic stainless steel by using FSW. The results of this study are listed below.

- Although tool of non-probe type is used in FSW butt welding for thin plate, FSW welded butt joints for thin plate with satisfactory acceptable joint strength is successfully achieved. It was observed that the maximum tensile strength was 450MPa with travel speed of 96mm/min and tool rotation speed of 900rpm.
- The hardness at the joints was higher than that of base metal due to strong shearing deformation and frictional heat affecting dynamic recrystallization. To be consider hardness distributions, the hardness of interface between base metal and joints was higher than that of base metal. It is thought that the regions of these hardness distributions probaly corresponds to heat affected zone(HAZ) or thermo-mechanically affected zone (TMAZ).

The width of the plastically deformed region decreased to vertical direction because frictional heat occur under the

- shoulder in this thin butt joints and frictional heat passes throughout inside. In comparison with back-up plate used, the stainless steel 430J1L of the same quality is superior to the Al alloy or mild steel at the depth of the plastically deformed

region. Also, the microstructure has a clear characteristic to optical microscope images in the way that it is hard to tell the heat affected zone (HAZ) and thermo-mechanically affected zone (TMAZ) respectively.

- In comparison with grain size of FSW welded butt joints for thin plate, the grain sizes of base metal were approximately average $20\mu\text{m}$. However, the grain sizes of butt joints decreased to about $5\mu\text{m}$, because the slightly finer recrystallized grain in the joint are attributed to the generation of strong shearing deformation and frictional heat affecting dynamic recrystallization.
- As a result of temperature history, the temperature of FSW welded butt joint near joint is lower than that of GTAW welded butt joint. Therefore, this temperature characteristics can be results in reduction of weld defects such as thermal deformation, residual stress etc.
- Moreover, tensile strength of end part of FSW Welded joint, which regarded as the weld defect was investigated. It was observed that end part of FSW Welded joint of thin plate indicated the good tensile strength which was 488MPa. It can be inferred that because of increasement of heat input by dwell time at end part.

References

- [1] G. Mallaiah, A Kumar, P. Ravinder Reddy, G Madhusudhan Reddy : Influence of grain refining elements on mechanical properties of AISI 430 ferritic stainless steel weldments – Taguchi approach, Journal of Materials and Design, 36, 443–450, 2012
- [2] M.O.H. Amuda, S. Mridha : Comparative evaluation of refinement in AISI 430 FSS welds by elemental metal powder addition and cryogenic cooling, Journal of Materials and Design, 35, 609–618, 2012
- [3] Mehmet Burak Bilgin, Cemal Meran : The effect of tool rotation and traverse speed on friction stir weldability of AISI 430 ferritic stainless steels, Journal of Materials and Design, 33, 376–383, 2012
- [4] Sigma phase embrittlement. In : ASM international handbook committee. ASM handbook – properties and selection irons steels and high performance alloy, vol. 1, p.1657, 1993
- [5] X.K. Zhu, Y.J. Chao : Numerical simulation of transient temperature and residual stresses in friction stir welding of 304L stainless steel, Journal of Materials Processing Technology, 146, 263–272, 2004
- [6] Sathiya P, Aravinda S, Noorul Haq A : Effect of friction stir welding parameters on mechanical and metallurgical properties of ferritic stainless steel joints, International Journal of advanced Manufacturing Technology, 31, 1076–1082, 2007

- [7] Lakshminarayanan Ak, Balasubramanian V : An assessment of microstructure, hardness, tensile and impact strength of friction stir welded ferritic stainless steel joints, Journal of Materials and Design, 31, 4592-4600, 2010
- [8] C Meran, O.E. Canyurt : Friction Stir Welding of austenitic stainless steels, Journal of Achievements in materials and Manufacturing Engineering, 43-1, 432-439, 2010

저작물 이용 허락서

학 과	선박해양공학과	학 번	20117095	과 정	석사
성 명	한글: 김 경 학 한문 : 金 京 鶴 영문 : Kyoung Hak, Kim				
주 소	전라남도 목포시 산정동 일신아파트 101동 803호				
연락처	E-MAIL : kimkh@chosun.ac.kr				
논문제목	(한글) 마찰교반접합기술을 이용한 박판 페라이트계 스테인리스강 접합부의 기계적 특성에 관한 연구 (영어) A Study on the Mechanical Characteristics of Friction Stir Welded Joints for Thin Ferritic Stainless Steel				

본인이 저작한 위의 저작물에 대하여 다음과 같은 조건아래 조선대학교가 저작물을 이용할 수 있도록 허락하고 동의합니다.

- 다 음 -

1. 저작물의 DB구축 및 인터넷을 포함한 정보통신망에의 공개를 위한 저작물의 복제, 기억장치에의 저장, 전송 등을 허락함
2. 위의 목적을 위하여 필요한 범위 내에서의 편집·형식상의 변경을 허락함. 다만, 저작물의 내용변경은 금지함.
3. 배포·전송된 저작물의 영리적 목적을 위한 복제, 저장, 전송 등은 금지함.
4. 저작물에 대한 이용기간은 5년으로 하고, 기간종료 3개월 이내에 별도의 의사 표시가 없을 경우에는 저작물의 이용기간을 계속 연장함.
5. 해당 저작물의 저작권을 타인에게 양도하거나 또는 출판을 허락을 하였을 경우에는 1개월 이내에 대학에 이를 통보함.
6. 조선대학교는 저작물의 이용허락 이후 해당 저작물로 인하여 발생하는 타인에 의한 권리 침해에 대하여 일체의 법적 책임을 지지 않음
7. 소속대학의 협정기관에 저작물의 제공 및 인터넷 등 정보통신망을 이용한 저작물의 전송·출력을 허락함.

동의여부 : 동의(O) 반대()

2013 년 2월

저작자 : 김 경 학 (서명 또는 인)

조선대학교 총장 귀하